



7N-2.8
193732
P-30

TECHNICAL NOTE

D-273

NUMERICAL COMPUTATION OF AERODYNAMIC

HEATING OF LIQUID PROPELLANTS

By John L. Kramer, Herman H. Lowell
and William H. Roudebush

Lewis Research Center
Cleveland, Ohio

NATIONAL AERONAUTICS AND SPACE ADMINISTRATION

WASHINGTON

April 1960

(NASA-TN-D-273) NUMERICAL COMPUTATION OF
AERODYNAMIC HEATING OF LIQUID PROPELLANTS
(NASA) 30 p

N89-70419

Unclas
00/28 0198732

NATIONAL AERONAUTICS AND SPACE ADMINISTRATION

TECHNICAL NOTE D-273

NUMERICAL COMPUTATION OF AERODYNAMIC

HEATING OF LIQUID PROPELLANTS

By John L. Kramer, Herman H. Lowell
and William H. Roudebush

SUMMARY

An application is made of one-dimensional aerodynamic heating theory to the calculation of heat input to rocket propellant tanks. The heat-transfer coefficient between the liquid propellant and the wall is included and is found to have a large influence in some cases. For example, in the zero insulation case the total heat input is more than doubled by neglecting the interior heat-transfer coefficient in the calculation. A detailed description of the numerical procedure is given, including a flow diagram to aid in digital computer programming. Results of several examples are presented.

The heat capacities of the insulation and the metal tank wall are not included. Examples are given which indicate the magnitude of the resulting error in several cases.

INTRODUCTION

The aerodynamic heating of missiles has been a major area of recent research. The engineering relations that have been developed are satisfactory for most calculations. For a discussion of two of the most widely used of these theories see references 1 and 2.

Most of the applications of the aerodynamic heating theory have been directed at obtaining skin temperatures. This information is required for the structural design of a missile and for protection of the payload under severe heating conditions.

With the increased use of cryogenic propellants attention must be paid also to the computation of the heat flow into these propellants. The actual failure of a mission or, at best, a large penalty in the form of superfluous insulation may accompany the failure to predict this heat

flow accurately. The calculation may require the inclusion of the heat-transfer coefficient on the propellant side of the tank as well as the other elements of the standard aerodynamic heating problem.

A numerical procedure for obtaining the heat input to a propellant under flight conditions was developed at the Lewis Research Center for use with a digital computer. Although the concepts and the equations used in the analysis are well known, a detailed outline of the calculation procedure may be useful to those wishing to make similar calculations. To facilitate engineering use of the method further, a block diagram is included to aid in computer programing.

The principal limitation of the method arises from the neglect of the heat capacity of the tank wall and the insulation. Such a quasi-steady treatment of the problem leads to increasing errors with increasing wall thicknesses. If the errors become unacceptably large, a second calculation is indicated to include, roughly, the effects of heat capacity.

ANALYSIS

Figure 1 is a schematic drawing of a section of propellant tank wall and insulation indicating the various temperatures and heating rates that enter the analysis. The heat flow through the aerodynamic boundary layer to the outer surface of the insulation is given by

$$q_{\text{ext}} = h_{\text{ext}} (T_r - T_1) \quad (1)$$

where T_r is the recovery temperature and T_1 is the temperature of the outside surface. Where there is no insulation T_1 becomes the temperature of the metal tank wall. Symbols are defined in the appendix.

The net heat flow into the insulation is given by

$$q = q_{\text{ext}} - q_{\text{rad}} = h_{\text{ext}} (T_r - T_1) - \epsilon \sigma T_1^4 \quad (2)$$

in which q_{rad} is the heat radiated away from the outer surface to an environment at 0°R .

Neglecting the heat capacity of the insulation the heat flow through the insulation is given by

$$q = \frac{k}{l} (T_1 - T_2) \quad (3)$$

where k is the mean conductivity of the insulation and l is the thickness. The assumption of no heat capacity results in a simplification of the problem. An indication of the effect of this assumption on the numerical results is given later.

The thermal resistance of the metal tank wall is so small compared with the thermal resistance of the insulation or of the external boundary layer that the temperature drop across the metal wall can be neglected. If, in addition, the heat capacity is neglected, no equation is necessary for the heat flow through the metal wall.

The heat flow into the liquid propellant is given by the equation

$$q = h_{liq} (T_2 - T_{liq}) \quad (4)$$

where T_{liq} is the bulk temperature of the liquid. In general not enough heat flows into a propellant tank to change the bulk temperature enough to affect calculations, so that T_{liq} can be assumed constant. The variation of h_{liq} with $T_2 - T_{liq}$, however, depends on the pressure in the propellant tank. The simplest case is the one in which the pressure is maintained constant so that only one curve of h_{liq} against $T_2 - T_{liq}$ is required. More general cases can be handled if h_{liq} as a function of $T_2 - T_{liq}$ and of tank pressure is available, and if a means for determining the tank pressure is provided.

Elimination of q from equations (2), (3), and (4) gives

$$h_{ext}(T_r - T_1) - \epsilon \sigma T_1^4 - \frac{k}{l} (T_1 - T_2) = 0 \quad (5)$$

and

$$h_{liq}(T_2 - T_{liq}) - \frac{k}{l} (T_1 - T_2) = 0 \quad (6)$$

The interior heat-transfer coefficient is generally determined experimentally for a given propellant. If T_{liq} is assumed constant, and if the tank pressure is known (either prescribed or calculated independently), then h_{liq} is essentially a function of T_2 :

$$h_{liq} = G(T_2) \quad (7)$$

The thermal conductivity of the insulation must also be determined experimentally. It is assumed that k can be expressed with sufficient accuracy in the form

$$k = a + b \left(\frac{T_1 + T_2}{2} \right) \quad (8)$$

where a and b are constants.

The substitution of equation (8) in equation (6) results in an equation quadratic in T_1 , the solution of which is

$$T_1 = -\frac{a}{b} + \left[\frac{a^2}{b^2} + T_2^2 + \frac{2}{b} (a + \lambda h_{liq}) T_2 - \frac{2\lambda T_{liq} h_{liq}}{b} \right]^{1/2} \quad (9)$$

Since a , b , and λ are fixed and h_{liq} is itself a function of T_2 , equation (9) can be written

$$T_1 = H(T_2) \quad (10)$$

With T_1 thus given as an explicit function of T_2 , equation (5) can be reduced by substitution to an equation involving only the variables h_{ext} , T_r , and T_2 :

$$h_{ext}[T_r - H(T_2)] - \epsilon \sigma [H(T_2)]^4 - \frac{1}{\lambda} \left[a + b \frac{T_2 + H(T_2)}{2} \right] [H(T_2) - T_2] = 0 \quad (11)$$

The adiabatic recovery temperature is related to the static temperature T_δ at the outer edge of the boundary layer by the equation

$$T_r = T_\delta \left[1 + r \frac{\gamma - 1}{2} M_\delta^2 \right] \quad (12)$$

and is independent of T_1 and T_2 . The recovery factor r is usually taken as 0.88 for turbulent airflow. The value of T_δ must be obtained from a knowledge of the flow field about the missile.

In some cases the ambient air temperature can be used in place of the local temperature T_δ . For accuracy, this requires that the point of calculation be sufficiently far downstream of the vehicle nose and that the tank walls are nearly cylindrical so that no large local pressure gradients exist. Furthermore, this approach neglects the bluntness effects described in reference 3.

The problem of determining the actual T_δ can be very difficult and will generally be done only in later stages of a vehicle design. However, if obtained, the correct values of T_δ can be used in the heat-transfer calculation as easily as the free-stream approximate values.

In the case that T_δ is approximated by the ambient air temperature, an ICAO standard atmosphere table such as reference 4 can be used.

The value of M_δ is obtained from the local air velocity at the outer edge of the boundary layer, or, analogously to the temperature, from the velocity of the vehicle when this latter affords an adequate approximation.

Thus, in the simplest cases, a knowledge of the trajectory is sufficient to determine T_r . For finer analyses the flow field about the vehicle must also be known.

The exterior heat-transfer coefficient appearing in equation (11) can be determined as a function of T_1 and certain parameters which are fixed in the calculation. The method used is that of reference 2 and is commonly referred to as a "reference temperature" method. Very simple relations can be obtained for compressible boundary layers providing the fluid properties are computed at a reference temperature. This temperature is determined through correlation of skin-friction data and is given in reference 2 in the form

$$T^* = T_\delta + 0.5 (T_1 - T_\delta) + 0.22 (T_r - T_\delta) \quad (13)$$

which is satisfactory for Mach numbers up to about 10. The fluid properties which must be evaluated at the reference temperature are given by

$$\left. \begin{aligned} k^* &= 0.753 \times 10^{-6} + 6.319 \times 10^{-9} T^* \quad (\text{ref. 5}) \\ \mu^* &= 0.231 \times 10^{-7} \left(\frac{(T^*)^{3/2}}{T^* + 216} \right) \quad (\text{ref. 6}) \\ \rho^* &= \rho_\delta \left(\frac{T_\delta}{T^*} \right) \\ \text{Re}^* &= \frac{\rho^* V x}{\mu^*} \end{aligned} \right\} \quad (14)$$

The length x is the distance along the surface from the stagnation point (always at the nose in this study) to the point of calculation (fig. 2).

Finally, the heat-transfer coefficient is given in terms of the fluid properties by

$$h_{\text{ext}} = 0.163 \frac{k^*}{x} \frac{\text{Re}^*}{(\log_{10} \text{Re}^*)^{2.584}} \quad (15)$$

At a given altitude and a fixed value of x equations (14) and (13) can be used with equation (15) to give h_{ext} as a function of T_1 . Then

from equation (10) h_{ext} becomes a function of the temperature T_2 alone:

$$h_{\text{ext}} = J(T_2) \quad (16)$$

Substitution of equation (16) into equation (11) gives

$$J(T_2)[T_r - H(T_2)] - \epsilon\sigma[H(T_2)]^4 - \frac{1}{l}\left[a + b \frac{T_2 + H(T_2)}{2}\right][H(T_2) - T_2] = 0 \quad (17)$$

containing the single unknown T_2 .

Equation (17) is the principal equation of the analysis. Because of the complex nature of the functions $J(T_2)$ and $H(T_2)$, a numerical solution is necessary. The Newton-Raphson method (ref. 7) proved to be satisfactory for the examples tried.

NUMERICAL PROCEDURE

A step-by-step description of the application of equation (17) to the missile propellant tank problem is given in this section. A block diagram is presented to facilitate programing for any automatic computer. A list of required input information and a list of quantities conveniently obtained in the process of solution are given.

The point on the tank at which the calculation is made is determined by the choice of the distance x (fig. 2). The total heat flow rate to the tank could have been obtained by computing the heat flow rates for several values of x and numerically integrating the result. It is much simpler, however, to compute the heat flow rate at some representative location and multiply by the wetted area. When a point halfway down the wetted area was selected as the representative location, it was determined in the numerical examples that the heat flow rate so calculated closely approximated what could be obtained by an integration over the wetted area.

Free-stream conditions are used throughout in place of local conditions at the outer edge of the boundary layer. This approximation is discussed in the section ANALYSIS.

The following is a list of the input data required for the computation:

(1) Trajectory

(a) Time from launch, sec

(b) Altitude, f

(c) Velocity, ft/sec

(d) Starting time of propellant flow from tank on which calculation is being made, sec

(2) Propellant tank

(a) Diameter, ft

(b) Distance from nose stagnation point to top of liquid at time zero, ft

(c) Insulation thickness, ft

(d) Thermal conductivity of insulation as linear function of $\frac{T_1 + T_2}{2}$, $\frac{\text{Btu}}{(\text{sq ft})(\text{sec})(^\circ\text{R}/\text{ft})}$

(e) Emissivity of outer surface

(3) Propellant

(a) Height of liquid at time zero, ft

(b) Flow rate, cu ft/sec

(c) Temperature, $^\circ\text{R}$

(d) Heat-transfer coefficient as function of T_2 , $\frac{\text{Btu}}{(\text{sq ft})(\text{sec})(^\circ\text{R})}$

A block diagram of the digital computer program is shown in figure 3. The diagram is explained by block number as follows:

(1) Compute initial wetted area, initial value of x , incremental changes in wetted area and x accompanying use of the propellant at the prescribed rate, and all constants used throughout the program.

(2) Read, or compute from trajectory equations, altitude and velocity of the vehicle as a function of time.

(3) Compute the free-stream static temperature and density from a data table (e.g., ICAO tables, ref. 4).

(4) Compute the recovery temperature from equation (12).

(5) Estimate the outside surface temperature T_1 by extrapolation of the results at previous altitudes. This decreases the time required for convergence of the numerical process. Of course at time zero there are no results at previous altitudes to use in the extrapolation process, but a first guess can be entered as input data with each problem or as a fixed constant in the program.

(6) Compute T^* from equation (13). Evaluate k^* , μ^* , ρ^* , and Re^* from equation (14).

(7) Compute h_{ext} from equation (15).

(8) Set T_2 equal to the propellant temperature T_{liq} , compute k from equation (8), and compute a new T_1 iterate using equation (5) and the Newton-Raphson formula (ref. 7).

(9) Compare the difference between two successive values of T_1 obtained by the Newton-Raphson process with a preestablished small number θ . If the process is determined not to have converged, return to step (6) and compute a new T^* (also k^* , μ^* , ρ^* , and Re^*) using the last approximation of T_1 . If the process has converged satisfactorily, the program proceeds to step (10).

(10) Compute q from equation (2).

(11) In general, the resistance to the heat flow offered by the propellant boundary layer is negligible unless film boiling occurs. For example, some data (ref. 8) for hydrogen at atmospheric pressure are shown in figure 4. For heat flow rates in the region of mild boiling ($q \leq 5.5 \text{ Btu}/(\text{sq ft})(\text{sec})$) the heat-transfer coefficients are greater than $1.0 \text{ Btu}/(\text{sq ft})(\text{sec})(^\circ\text{R})$. When film boiling occurs ($q > 5.5 \text{ Btu}/(\text{sq ft})(\text{sec})$) the heat-transfer coefficients are less than $0.1 \text{ Btu}/(\text{sq ft})(\text{sec})(^\circ\text{R})$.

The inner wall temperature (for a constant tank pressure) is seen to change, at the most, a few degrees if the heat input rate is insufficient to cause film boiling. For this reason it is convenient to start the analysis (as in step (8)) by setting the inner wall temperature equal to the propellant temperature. Once a heat flow rate has been computed based on this assumption, it can be compared with the rate required for film boiling to occur. If film boiling is indicated not to occur, the error in the heat flow rate caused by the inaccuracy of a few degrees in the inner wall temperature is negligible. However, if film boiling does occur, that is, if the calculated heat flow rate is sufficient to support film boiling, the heat flow rate must be recalculated including now the thermal resistance (no longer negligible) associated with the interior heat-transfer coefficient given in figure 4.

A vehicle will, in general, begin its flight without film boiling occurring. As speed increases, film boiling may occur. When this happens the program should switch itself from a calculation sequence predicated (in effect) on an infinitely great interior heat-transfer coefficient to the general sequence which takes into account a finite interior heat-transfer coefficient.

It is possible, of course, to include a finite h_{liq} for all calculations, including those for which no film boiling occurs. The more complicated form of the h_{liq} curve in the region of small $T_2 - T_{liq}$, however, caused serious difficulties in the numerical process. The Newton-Raphson method actually diverged in some cases, and no method could be found of general acceptability.

In step (11), therefore, the heat flow rate is compared with the rate indicated by the data to be required for film boiling. If film boiling does occur, proceed to step (12); otherwise proceed to step (19).

(12) Estimate the wall temperature T_2 . This can be done by extrapolation of results at previous altitudes. (See step (5) for starting procedure.)

(13) Compute h_{liq} from an analytical expression approximating the film boiling region in figure 4, or use discrete h_{liq} data with an interpolation procedure.

(14) Solve equation (9) for T_1 , using the T_2 of step (12). Repeat steps (6) and (7) with this value of T_1 .

(15) Compute a new T_2 iterate using equation (17) and the Newton-Raphson formula.

(16) Test successive approximations of T_2 for convergence. If satisfactory convergence has occurred, proceed to step (17); otherwise return to step (13).

(17) Test $T_2 - T_{liq}$ against a predetermined value to decide whether film boiling occurs. At some point along the trajectory the heat flow rate will become so low that the vapor film will collapse and the resistance of the propellant to the heat flow will again become negligible. When this occurs the program adjusts itself to set T_2 equal to T_{liq} for this and all subsequent calculations and returns to step (6) using the last value of T_1 computed from equation (9). If the film is found to exist the program proceeds to step (18).

(18) Compute h_{liq} from the final value determined for T_2 in step (15).

(19) Compute correct values of h_{ext} , q , and the total heat input.

(20) Punch desired quantities and return to step (2) for the next point on the trajectory.

Quantities occurring in the calculation and having potential interest are the following:

- (1) Altitude, velocity, time
- (2) Total heat input
- (3) Heat flow rate from aerodynamic boundary layer
- (4) Heat radiated from outer surface
- (5) Heat flow rate into propellant
- (6) External heat-transfer coefficient
- (7) Recovery temperature, reference temperature, and outer and inner wall surface temperatures
- (8) Reference Reynolds number and free-stream Mach number

EXAMPLES

The digital computer program outlined in the preceding section has been applied to several trajectories to determine the associated heat flow rate into the liquid propellants. For the purpose of illustrating the effect of the interior heat-transfer coefficient, a single trajectory with several insulation thicknesses is considered.

A two-stage missile is used for the calculation. The first stage is a solid-propellant booster with an average thrust of about 120,000 pounds. The second stage is a liquid-hydrogen - liquid-oxygen combination with an average thrust of about 12,000 pounds. The burning time for the first stage is 26 seconds, including 2 seconds of thrust decay. This is followed by 26 seconds of burning time for the second stage. The altitude and velocity histories are presented in figures 5 and 6.

The calculation is made for the hydrogen tank of the second stage of the missile. The curve of figure 4 is used for the interior heat-transfer coefficient, assuming a constant pressure in the propellant

tank. The insulation used for the examples has a thermal conductivity given by

$$k = 0.0287 \times 10^{-4} + 0.02315 \left(\frac{T_1 + T_2}{2} \right) \times 10^{-7}$$

and an emissivity of 0.6. The tank has a diameter of 2.67 feet and an initial liquid depth of 5.98 feet. The flow rate from the hydrogen tank is 5.65 pounds per second. The distance from the stagnation point (nose) to the surface of the hydrogen is 9.84 feet at zero time. A recovery factor of 0.88, typical of turbulent airflow, is used in equation (12).

To compute the total heat flow rate, a local heat flow rate was first computed at a point on the hydrogen tank at the midpoint of the fluid depth. This rate was then multiplied by the wetted area in the hydrogen tank at the time in question. As the hydrogen is used up in the second stage of the flight, the effective heating area (the wetted area) decreases and cuts down the total heat flow rate. Figure 7 shows both the local heat flow rate and the total heat flow rate (the local rate times the wetted area) for the case of zero insulation thickness. The total heat flow rate falls off to zero as the propellant is consumed and the wetted area decreases to zero.

The first example assumes no insulation. The resistance of the propellant boundary layer to the flow of heat is negligible compared with that of the air boundary layer in all cases where film boiling does not occur. With the trajectory chosen for this example, film boiling does occur within the first 2 seconds of flight, and the resistance of the vapor film can not be ignored. Figure 8(a) shows the total heat flow rates into the hydrogen tank computed, in the first case, by assuming an infinite value of heat-transfer coefficient (zero resistance) in the hydrogen, and secondly, by taking the appropriate values of heat-transfer coefficient from the data of figure 4. The difference in the two results is substantial and could not be ignored in most engineering calculations. The total heat input (the integral of the curve in fig. 8(a)) computed using an infinite heat-transfer coefficient is more than twice the value computed using the finite coefficient.

Figure 8(b) gives the outer surface temperatures calculated using the correct hydrogen heat-transfer coefficient. Assuming an infinite heat-transfer coefficient would imply that the metal wall was itself at the temperature of the liquid hydrogen. Such a result would be useless.

The second example assumes an insulation thickness of 0.005 inch. Although this thickness is not practical, except perhaps for a sprayed insulation, it provides an example of delayed film boiling. For the first 22 seconds of flight the heat flow rate is not large enough to cause a hydrogen vapor film to develop. Figure 9(a) shows the heating

rate computed with infinite hydrogen heat-transfer coefficient, as well as that computed using the data of figure 4. At about 22 seconds the curves diverge rapidly as the resistance of the film cuts down the heat flow into the propellant. As time passes the difference in h_{liq} is overcome by the diminishing size of the wetted area, and both curves approach zero as the tank empties. The total heat input obtained by assuming an infinite value of h_{liq} in this case is about 1.1 times the correct value. An error of this magnitude is hardly significant in such an approximate calculation as the present one. However, it is indicated that h_{liq} cannot be ignored in more refined calculations if film boiling can be expected to occur somewhere along the flight path.

Figure 9(b) shows the outside surface temperatures for the two cases. Using an infinite h_{liq} results in maximum surface temperatures which are about 10 percent too low.

Insulation thicknesses of 0.010 and 0.10 inch were also used in the computations. No film boiling occurs for these thicknesses, and therefore an infinite value of h_{liq} is a good assumption. The total heat flow rates for the two cases are shown in figure 10(a). The outside surface temperatures are shown in figure 10(b).

DISCUSSION

The calculations, as described in this report, can be made quickly, less than 2 minutes being required for a complete trajectory on the IBM 704. The speed and ease of calculation makes the method useful in mapping out areas of interest and danger in the use of cryogenic propellants. The simplifying assumptions, however, must be understood in order that the limitations of the method are kept clearly in mind.

The use of a one-dimensional heat flow equation limits the calculation to those areas where large temperature gradients along the tank wall do not exist. For obtaining gross heat-transfer effects on propellant tanks, this is probably not a serious limitation. However, the method may prove inadequate in the regions of interest from a stress analysis standpoint.

The use of free-stream conditions in the place of local conditions at the edge of the boundary layer can lead to significant errors if the calculation is made close to the nose or in a region of large curvature. A substantial change in total pressure due to a strong shock can also lead to a discrepancy, but such a change can be included without serious additional effort. This is not the case with the actual local conditions, the determination of which is sometimes a very difficult job.

Perhaps the most significant limitation arises from neglecting the heat capacity of the insulation and of the metal tank wall. The resulting error increases with increasing thicknesses of metal and insulation. Even for thin walls the effect can be significant when film boiling occurs sometime after the flight has begun, as in figure 9. The inner wall temperature T_2 is required to rise very substantially as the vapor film develops. The rate at which this rise can take place is not infinite, and the inclusion of the heat capacity of the metal tank wall in the calculation does produce noticeable differences in T_2 as a function of time.

To investigate the effect of the heat capacity in the present examples, a simplified numerical analysis was carried out based on the h_{ext} values of the original computation. These values are slightly in error, since the outer surface temperature changes when heat capacity is included. However, the error will be small, and quite a simplification is realized in this way.

Including only the heat capacity of the insulation resulted in the outer surface temperatures and heat flow rates shown in figure 11 for 0.10 inch of insulation. The effect on the outside surface temperature (fig. 11(a)) is mainly a time shift with the maximum temperature almost the same in the two cases. The effect on the local heat-transfer rate (fig. 11(b)) is also a shift, but the result is much more significant. The reason for this is that the high heat inputs are delayed in time by including heat capacity, and their effect on the total heat flow rate is diminished by the decreased wetted area (fig. 11(c)). The result is that the total heat input (area under the curve in fig. 11(c)) is decreased from 846 Btu in the case of no heat capacity to 596 Btu in the case where heat capacity is included. It is clear that if the level of the hydrogen had not been decreasing this difference would not have been so large.

A calculation was also made for 0.01 inch of insulation, and no change from the original results was obtained when heat capacity was included. In this case the heat capacity of the insulation could be ignored with no error.

Another set of calculations was made for 0.005 inch of insulation which included the heat capacity of the metal tank wall (neglecting the heat capacity of the insulation which was expected to have no effect in this case). This case was chosen because the occurrence of film boiling calls for an abrupt rise in metal tank wall temperature (fig. 12(a)). Figure 12(a) also shows the tank wall temperature when heat capacity is included in the calculation. The resulting temperature rise is slower, and the heat flow rates will be correspondingly lower in this region (fig. 12(b)). On the other hand, including the heat capacity causes the heat flow rates to decrease more slowly in the latter part of the flight. The net effect on the total amount of heat input is a decrease from 7713 Btu

in the case of no heat capacity to 7528 Btu in the case where heat capacity was included.

In view of the above results, care must be used in the application of the method. However, a wide range of engineering calculations do fall within its proper scope.

Lewis Research Center
National Aeronautics and Space Administration
Cleveland, Ohio, January 4, 1960

APPENDIX - SYMBOLS

a,b	constant coefficients in eq. (8)
G,H,J	functions
h_{ext}	exterior heat-transfer coefficient, Btu/(sq ft)(sec)(°R)
h_{liq}	liquid propellant heat-transfer coefficient, Btu/(sq ft)(sec)(°R)
k	thermal conductivity of insulation, Btu/(sq ft)(sec)(°R/ft)
k^*	thermal conductivity of air evaluated at reference temperature T^* , Btu/(sq ft)(sec)(°R/ft)
l	insulation thickness, ft
M_δ	Mach number at outer edge of boundary layer
q	specific rate of heat flow into propellant, Btu/(sq ft)(sec)
q_{ext}	specific rate of heat flow from boundary layer, Btu/(sq ft)(sec)
q_{rad}	heat radiated from outside surface, Btu/(sq ft)(sec)
Re^*	Reynolds number evaluated at reference temperature T^*
r	recovery factor
T_{liq}	liquid propellant temperature, °R
T_r	recovery temperature, defined by eq. (12), °R
T_1	outside surface temperature, °R
T_2	metal wall temperature, °R
T_δ	temperature at outer edge of boundary layer, °R
T^*	reference temperature, defined by eq. (13), °R
V	flight velocity, ft/sec
x	distance from nose stagnation point to point of calculation, ft

γ	ratio of specific heats of air
ϵ	emissivity of outside wall
θ	preestablished temperature difference for determining convergence
μ^*	viscosity of air evaluated at reference temperature T^* , (lb)(sec)/sq ft
ρ_δ	density of air at outer edge of boundary layer, slugs/cu ft
ρ^*	density of air evaluated at reference temperature T^* , slugs/cu ft
σ	Stefan-Boltzman constant, 4.8×10^{-13} Btu/(sq ft)(sec)($^{\circ}\text{R}^4$)

REFERENCES

1. Van Driest, E. R.: The Problem of Aerodynamic Heating. Aero. Eng. Rev., vol. 15, no. 10, Oct. 1956, pp. 26-41.
2. Eckert, E. R. G.: Engineering Relations for Heat Transfer and Friction in High-Velocity and Turbulent Boundary-Layer Flow over Surfaces with Constant Pressure and Temperature. Trans. ASME, vol. 78, no. 6, Aug. 1956, pp. 1273-1283.
3. Moeckel, W. E.: Some Effects of Bluntness on Boundary-Layer Transition and Heat Transfer at Supersonic Speeds. NACA Rep. 1312, 1957. (Supersedes NACA TN 3653.)
4. Minzner, R. A., Ripley, W. S., and Condron, T. P.: U.S. Extension to the ICAO Standard Atmosphere - Tables and Data to 300 Standard Depotential Kilometers. U.S. Govt. Printing Office, 1958.
5. Keenan, Joseph H., and Kaye, Joseph: Thermodynamic Properties of Air. John Wiley & Sons, Inc., 1947.
6. Ames Research Staff: Equations, Tables, and Charts for Compressible Flow. NACA Rep. 1135, 1953. (Supersedes NACA TN 1428.)
7. Scarborough, James B.: Numerical Mathematical Analysis. Second ed., The Johns Hopkins Press, 1950.
8. Mulford, Robert N., and Nigon, Joseph P.: Heat Exchange Between Copper Surface and Liquid Hydrogen and Nitrogen. LA-1416, Tech. Info. Service, U.S. Atomic Energy Comm., May 21, 1952.

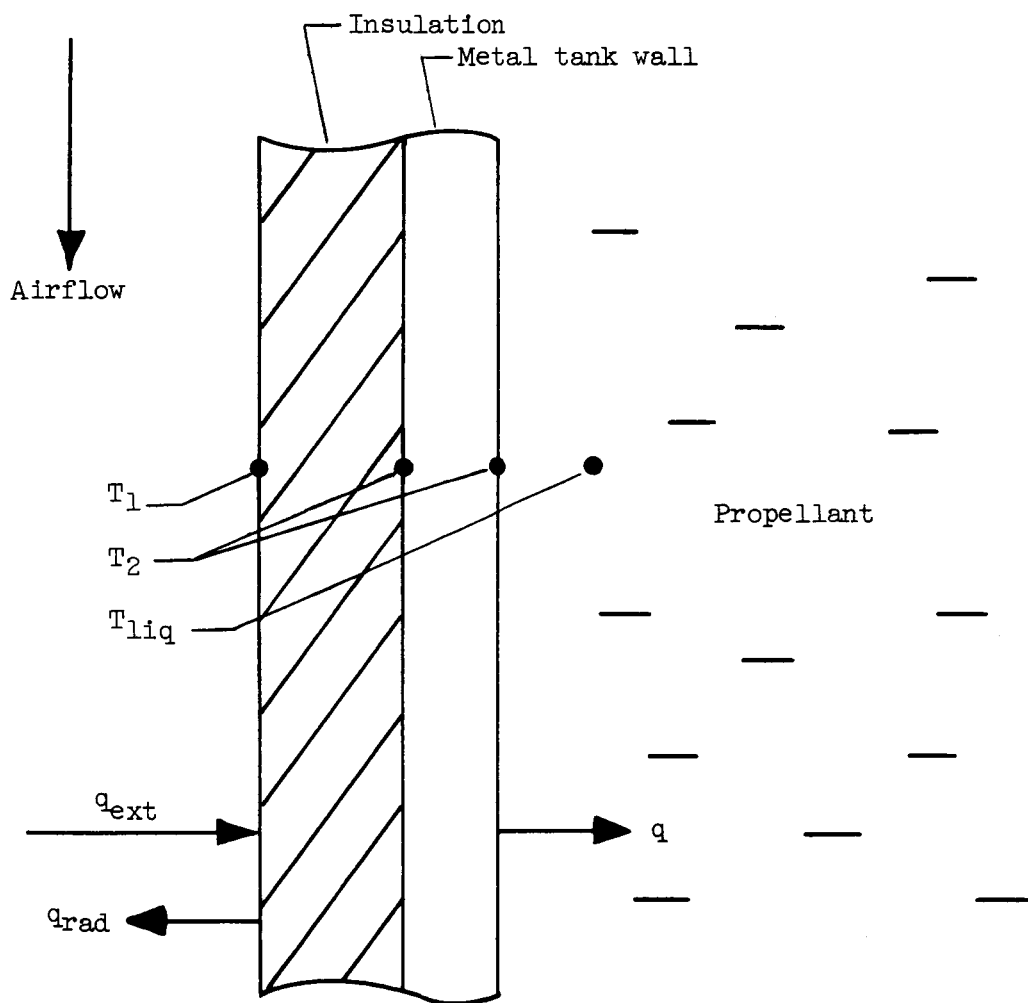


Figure 1. - Tank wall section with heat flux and pertinent temperatures indicated.

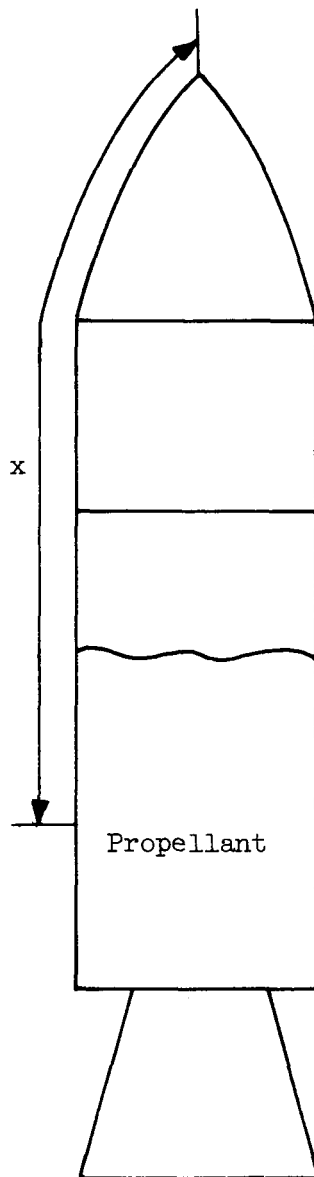


Figure 2. - Schematic drawing of missile indicating distance x used in analysis.

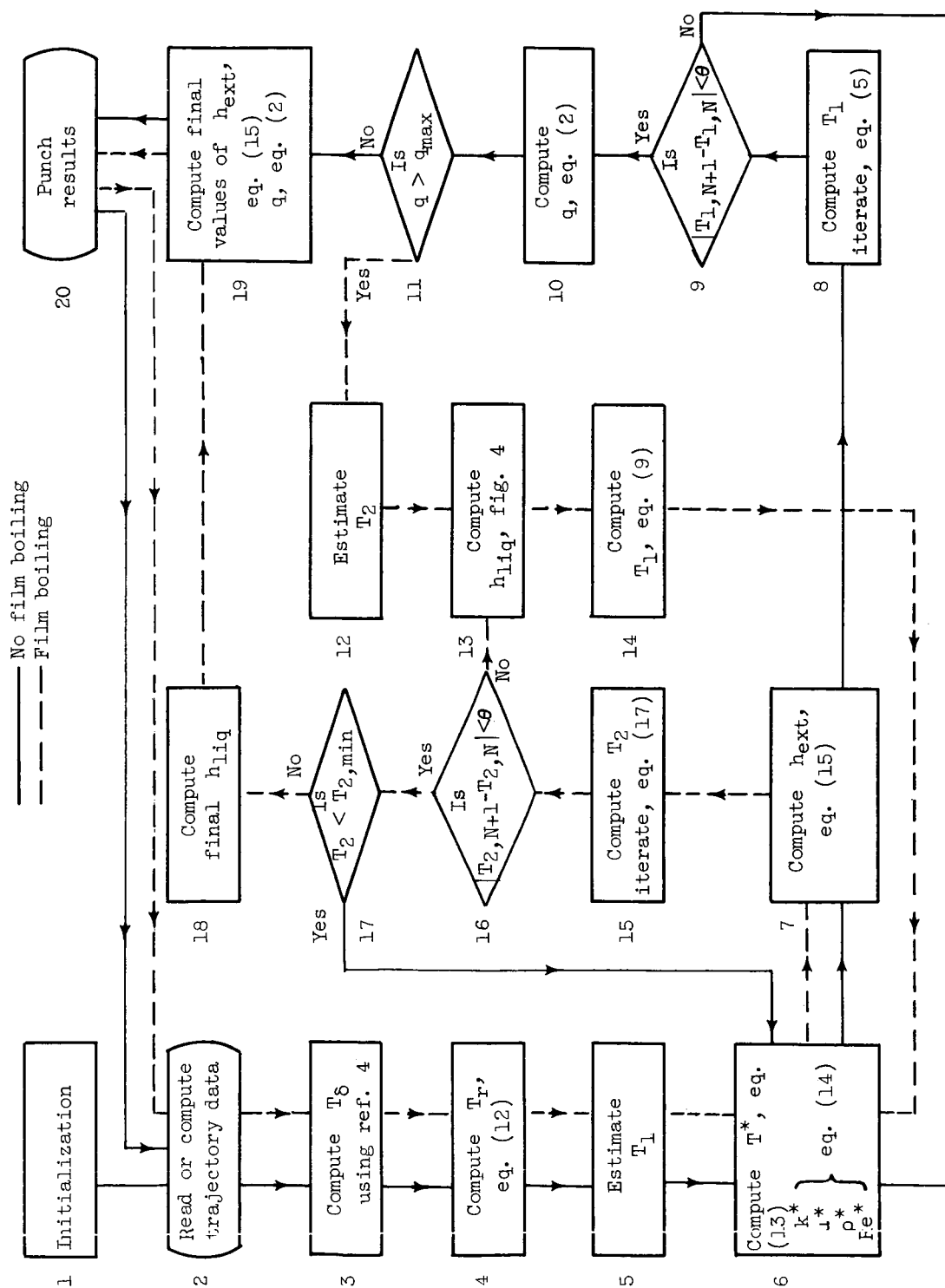


Figure 3. - Diagram for computer program.

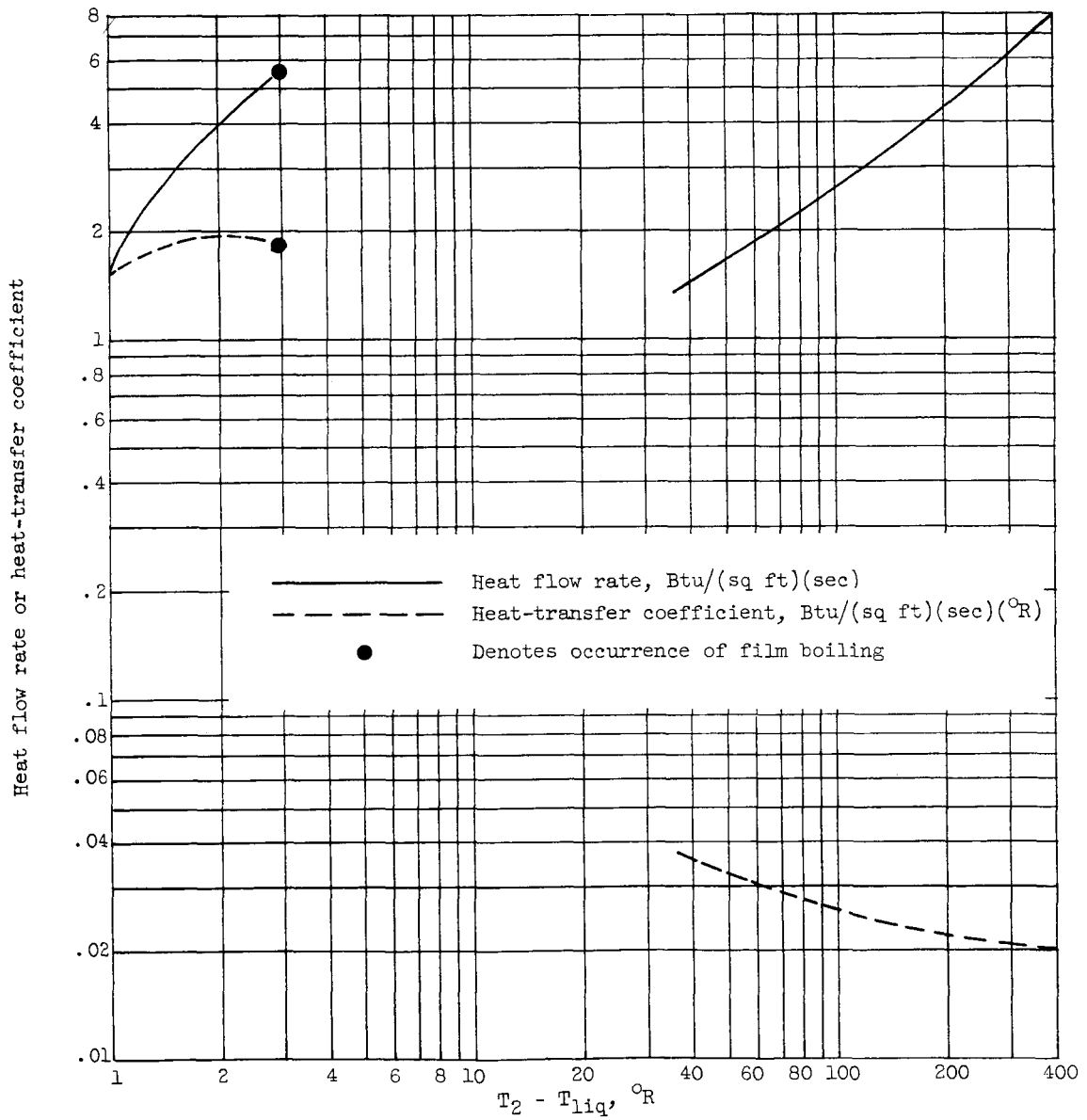


Figure 4. - Heat flow rate and heat-transfer coefficient for liquid hydrogen (ref. 8).

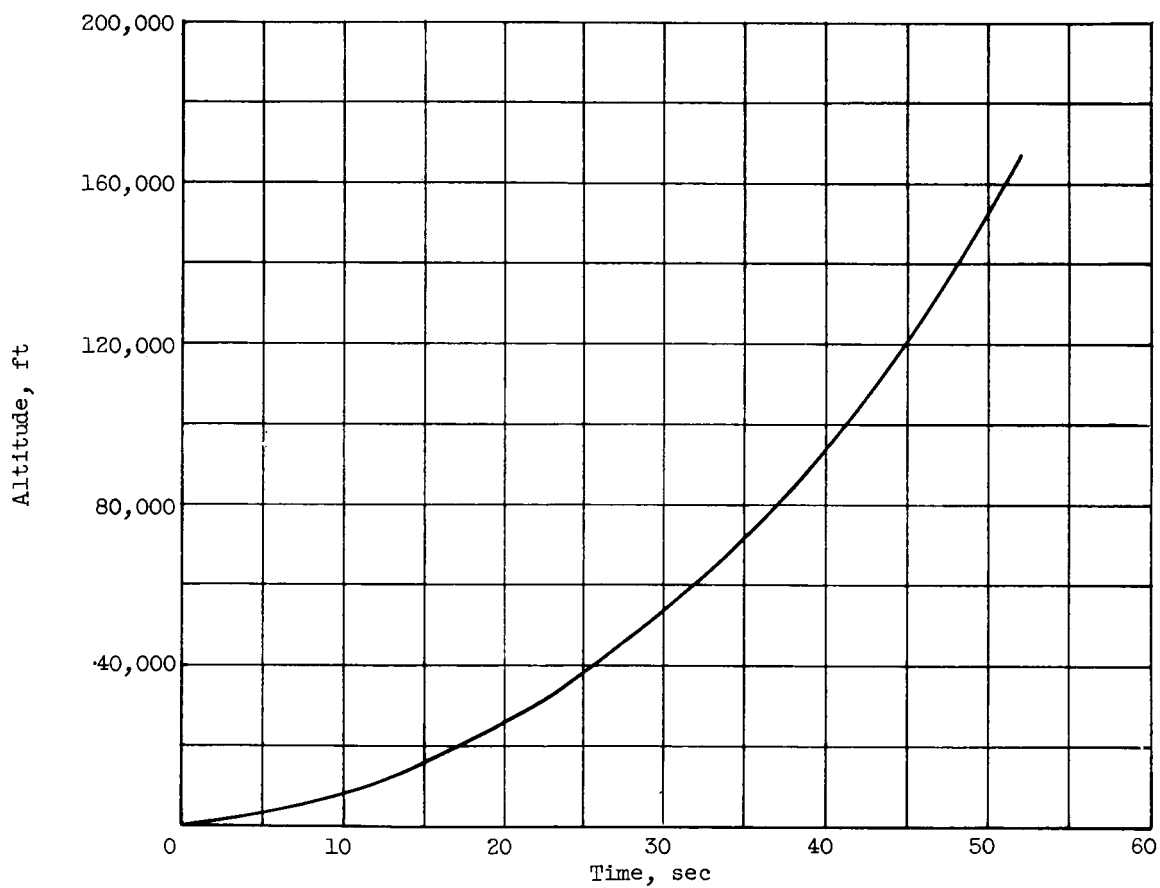


Figure 5. Altitude as a function of time.

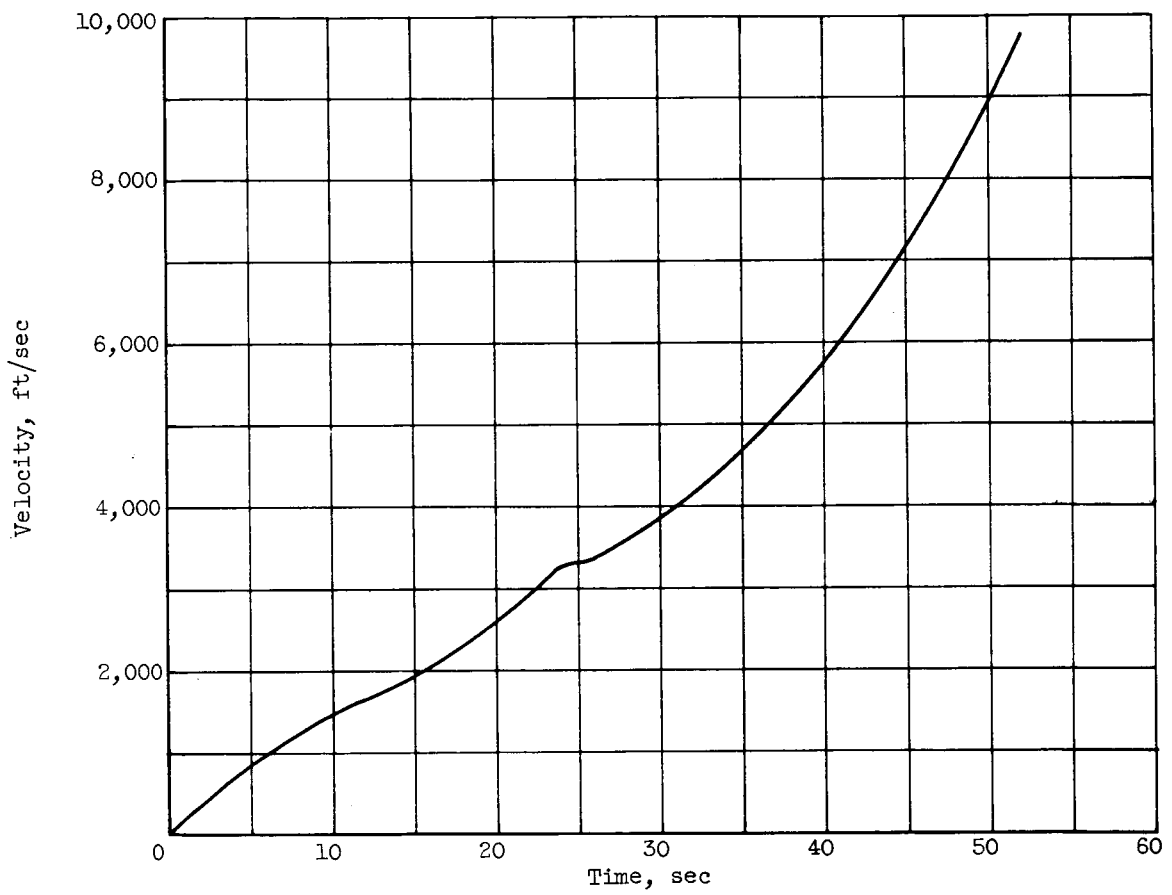


Figure 6. - Velocity as a function of time.

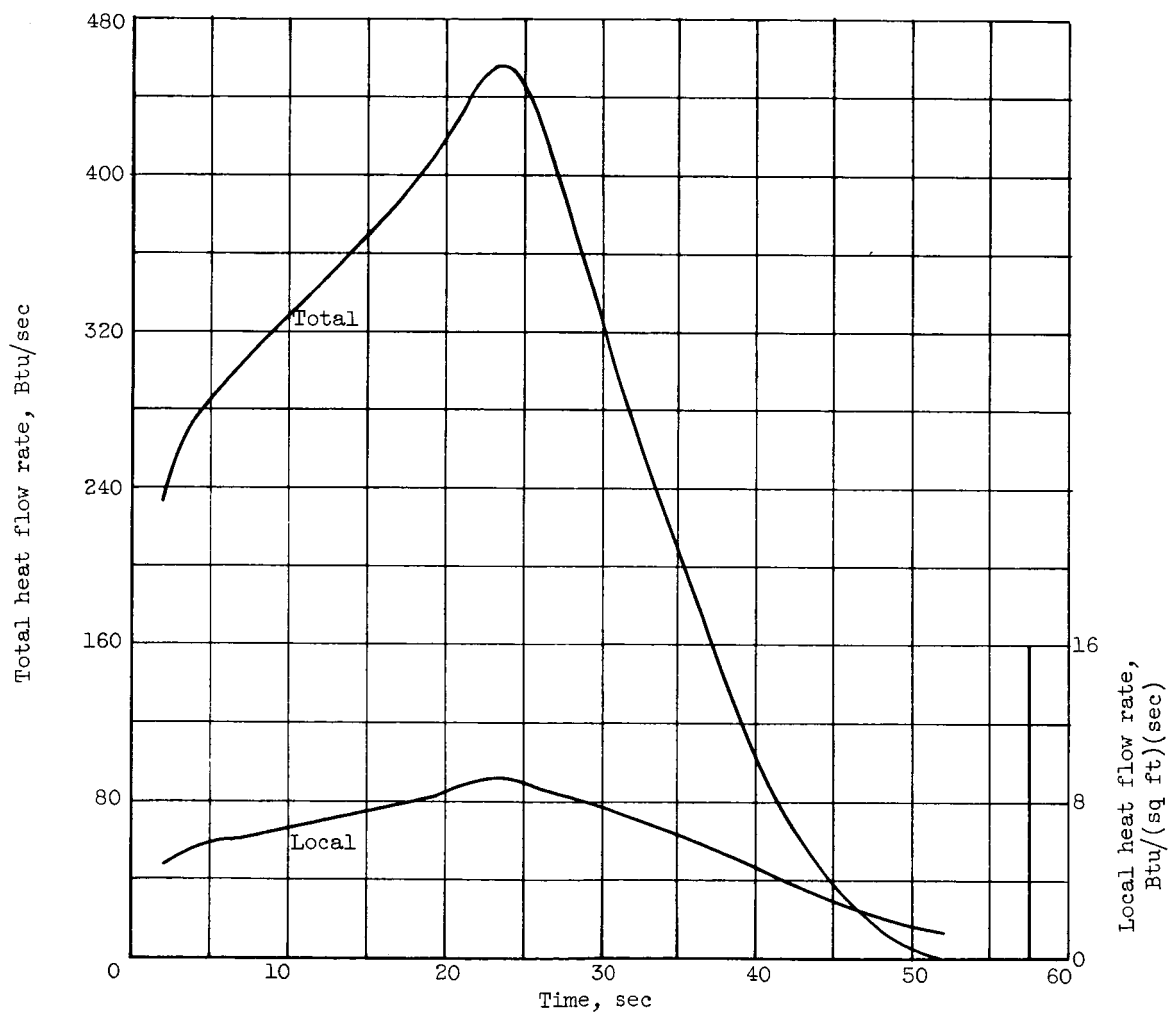
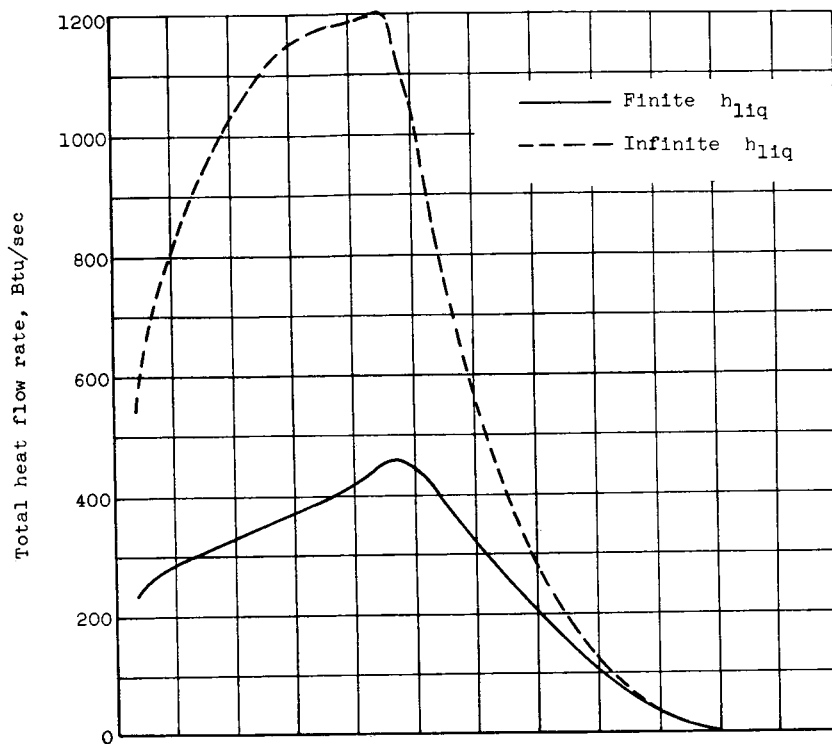
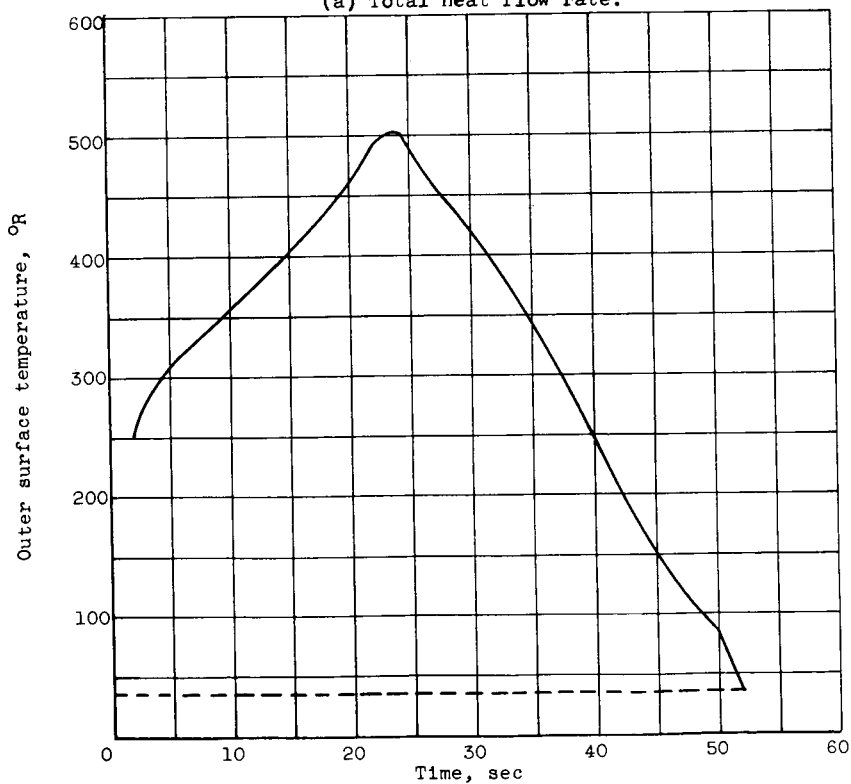


Figure 7. - Comparison of local heat flow rate with total heat flow rate (local rate times wetted area).



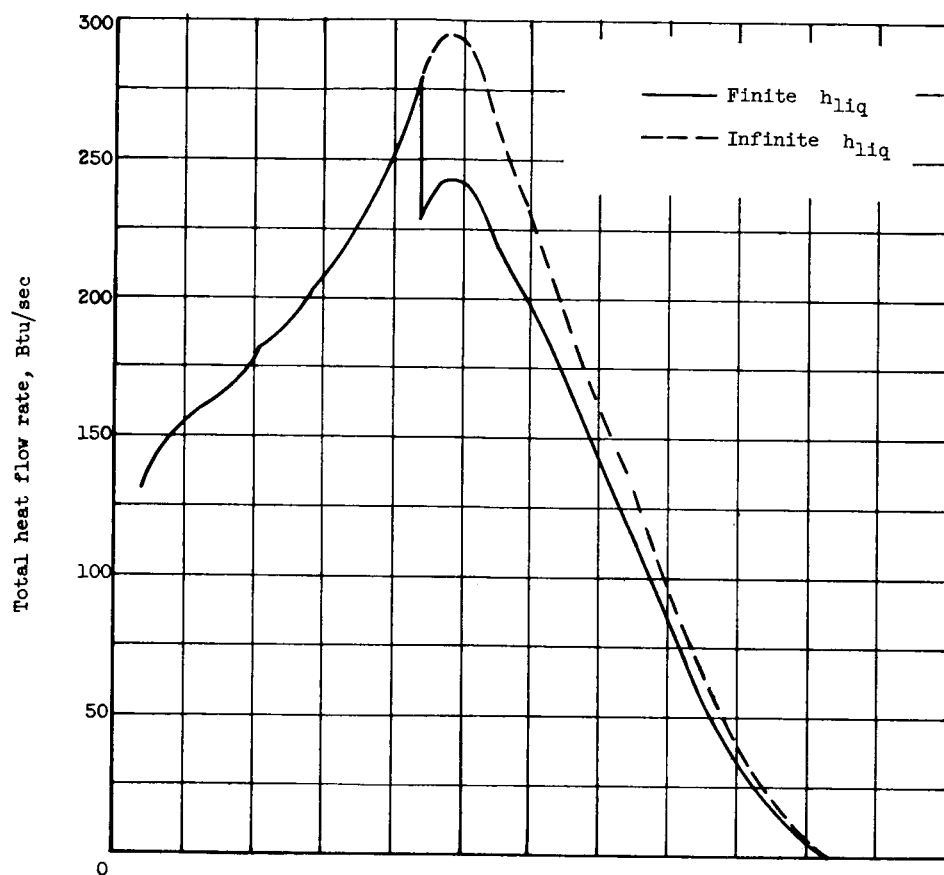
(a) Total heat flow rate.



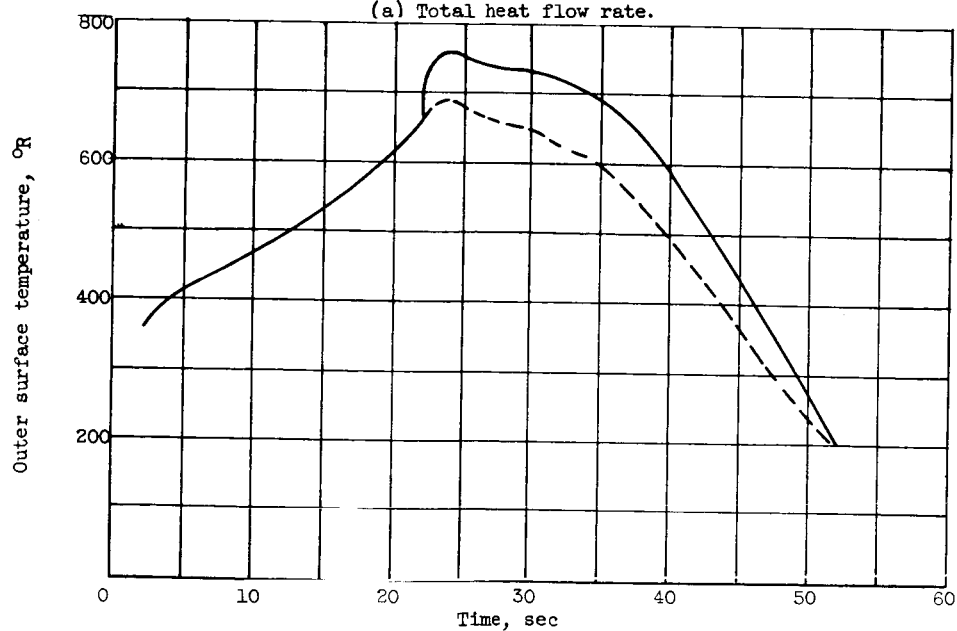
(b) Outer surface temperature.

Figure 8. - Data for tank with insulation of zero thickness.

E-609

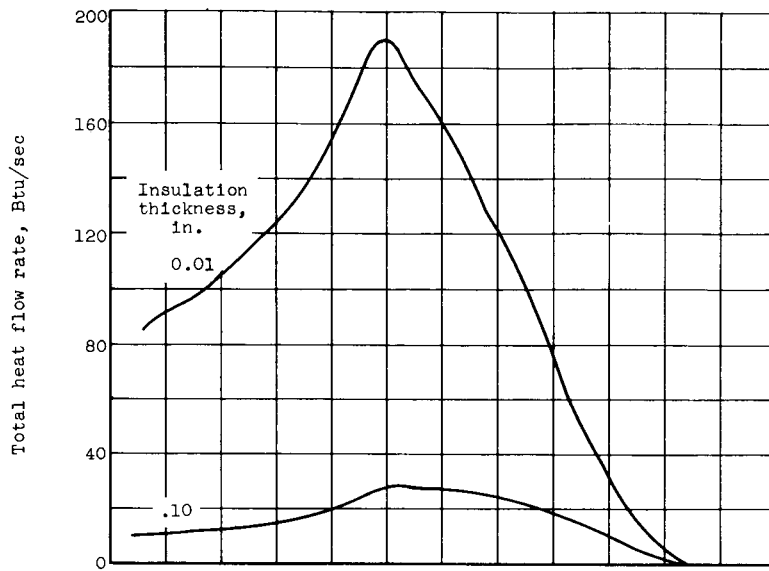


(a) Total heat flow rate.

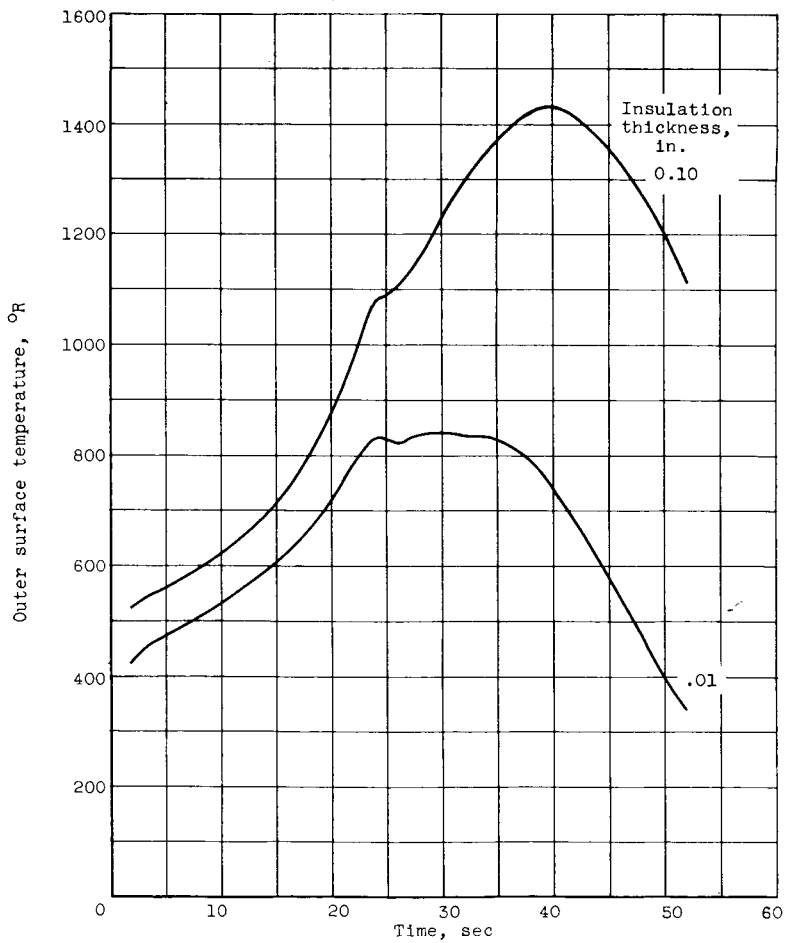


(b) Outer surface temperature.

Figure 9. - Data for tank with insulation 0.005 inch thick.



(a) Total heat flow rate.



(b) Outer surface temperature.

Figure 10. - Data for tank with insulation 0.01 and 0.1 inch thick.

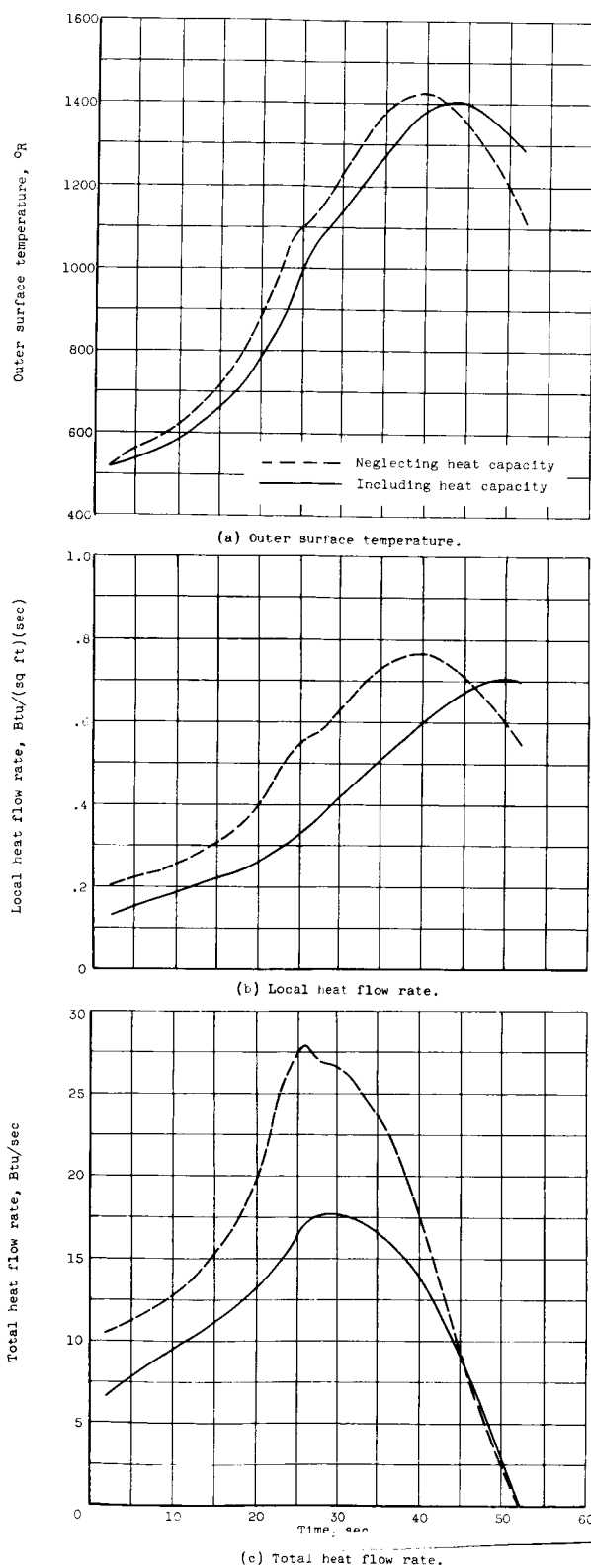
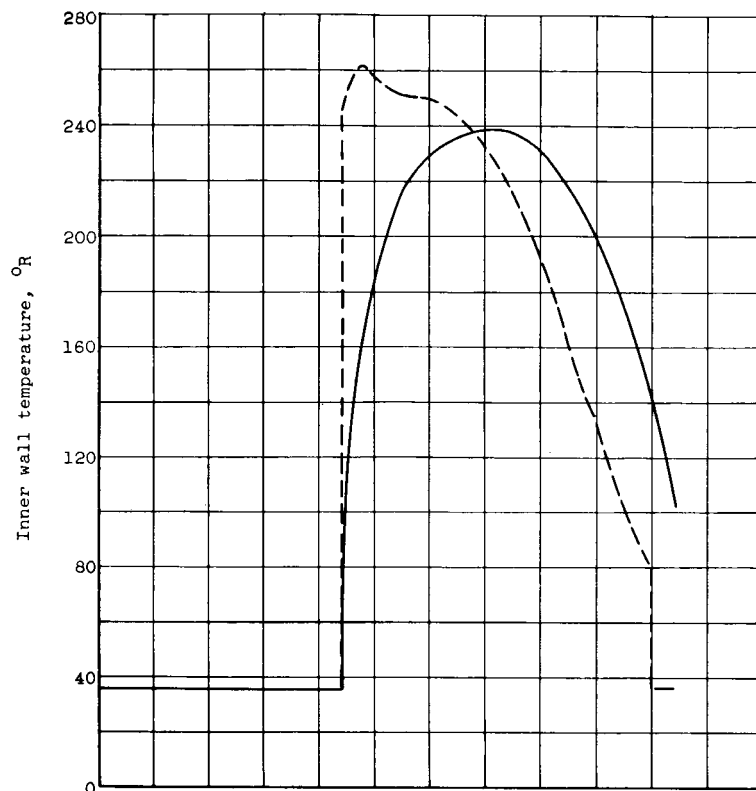
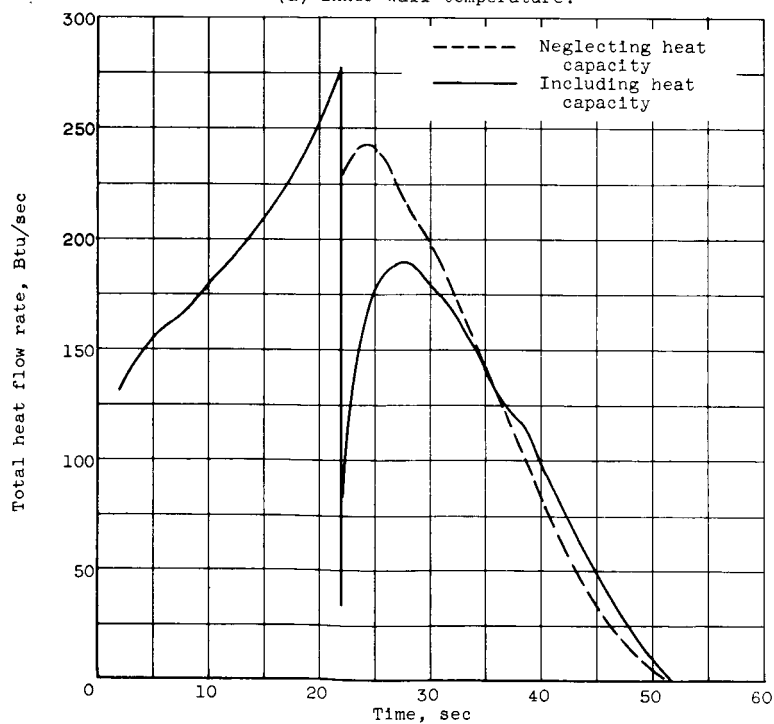


Figure 11. - Data for tank with insulation 0.1 inch thick with heat capacity neglected and included.



(a) Inner wall temperature.



(b) Total heat flow rate.

Figure 12. - Data for tank with aluminum wall 0.070 inch thick and insulation 0.005 inch thick.